XX ICongresso Brasileiro de Mecânica dos Solos e Engenharia Geotécnica
X Simpósio Brasileiro de Mecânica das Rochas
X Simpósio Brasileiro de Engenheiros Geotécnicos Jovens
24 a 27 de setembro de 2024 – Balneário Camboriú/SC

COBRAMSEG 2024
XXI Congresso Brasileiro de Mecânica dos Solos e Eng. Geotécnica
X Simpósio Brasileiro de Mecânica das Rochas
X Simpósio Brasileiro de Engenheiros Geotécnicos Jovens

Iron Ore Tailings Critical State Properties from Basic Laboratory Tests for Static Liquefaction Analysis

Ccotohuanca, Jose
Geotechnical Engineer, Klohn Crippen Berger, Belo Horizonte, Brazil, jccotohuanca@klohn.com

Lanza, Vinícius
Engineering Assistant, Klohn Crippen Berger, Belo Horizonte, Brazil, vlanza@klohn.com

Costa, Isabella
Engineering Assistant, Klohn Crippen Berger, Belo Horizonte, Brazil, icosta@klohn.com

Ninanya, Hugo
Senior Geotechnical and Hydrogeological Engineer, Klohn Crippen Berger, Belo Horizonte, Brazil, hninanya@klohn.com

ABSTRACT: In the last nine years, Brazil experienced two significant tailings storage facility (TSF) failures: the rupture of Fundão TSF in Mariana (2015) and TSF I in Brumadinho (2019). After these incidents, new legislative measures were proposed, introducing the concept of "TSF decharacterization". Moreover, the failures prompted increased interest in filtered tailings stacks. As part of decharacterization and filtered projects, comprehensive geotechnical testing campaigns have been carried out, mainly focused on studying the mechanical behavior of tailings using the Critical State Soil Mechanics (CSSM) with the Critical State Locus (CSL) representing a mean of assessing tailings strength-deformation characteristics. A substantial database of critical state (CS) parameters has been developed and published mainly on iron ore tailings, as most iron ore TSFs are situated within the Iron Quadrangle in Brazil. The unique features of these tailings, marked by a high iron content contributing to a high specific gravity (G_s), render conventional geotechnical correlations not applicable without further considerations. This article compiles CS parameters of 35 iron ore tailings from various locations. These parameters are then compared to basic laboratory data, such as fines content (FC), average particle size (D_{50}), Atterberg limits, iron content, and so forth. The aim is to establish correlations between basic iron ore tailings data and CS parameters, providing a screening approach to determine if laboratory results are within expected ranges when evaluating static liquefaction for iron ore TSFs.

KEYWORDS: Iron ore tailings, Critical State Soil Mechanics, Critical State Line, index parameters, static liquefaction.

1 INTRODUCTION

Static liquefaction is defined as sudden strength loss in a (near) saturated (typically granular) soil, accompanied by rapid generation of excess pore-water pressure. This could develop into a liquefaction flow failure if the soil strength drops below the applied shear stress (Lade and Yamamuro, 1997). Recent incidents, such as the failures at Fundão (Morgenstern et al., 2016) and Brumadinho (Robertson et al., 2019), have identified static liquefaction as a primary failure mechanism. Such Brazilian TSF failures have resulted in unprecedented and devastating consequences for the environment, infrastructure damage and human losses. In response, new regulations have been enacted in Brazil, introducing the concept of TSF decharacterization. The failures also spurred increased interest in alternative dewatered tailings technologies (e.g. filtered tailings), due to their lower risk compared to conventional hydraulically deposited tailings.

In the Brazilian context, where decharacterization and filtered tailings projects were not commonly practiced, comprehensive geotechnical investigations were required to understand the behaviour of the tailings material to support static liquefaction assessment, generally following the critical state soil mechanics (CSSM)

framework. Consequently, a database of critical state (CS) parameters was developed and published primarily on iron ore tailings, given the predominant location of TSF within the Iron Quadrangle in Brazil, an area renowned for hosting one of the world's largest reserves of iron ore.

While it is widely recognized that soil index properties impact critical state locus (CSL) parameters (Jefferies and Been, 2015), research linking tailings index properties to CSL parameters remains limited. Smith et. al. (2019), Torrez-Cruz and Santamarina (2020), Macedo and Vergaray (2022) and Hussien and Sgaoula (2023) are among the few related studies. However, no investigation targeting tailings from a unique commodity (iron ore in this study) has been identified.

This article aims to provided trends between CS parameters and iron ore tailings index properties including specific gravity (G_s), fines content (FC), mean particle size (D_{50}), coefficient of uniformity (C_u), Atterberg limits represented by the plasticity index (PI) and liquid limit (LL), minimum (e_{min}) and maximum (e_{max}) void ratios as well as the iron oxide content. A database was compiled incorporating 35 iron ore tailings materials from Brazil and various global mining sites. This database, along with the correlations found, offer a valuable screening approach to discern whether laboratory results are within expected ranges or if more detailed tests are required when assessing static liquefaction for iron ore TSFs.

2 IRON ORE TAILINGS DATABASE

The iron ore tailings database ("the IOD") consists of 35 iron ore tailings sources from several mines located throughout Brazil, Australia, and China; 9 of them as part of this study and the rest from published literature as detailed in Table 1. The IOD includes index properties along with CSL parameters, including: the slope on a natural logarithm base ($\lambda_e = \lambda_{10}/2.3$) and the altitude at 1 kPa (Γ), when the CSL is represented by a linear function using a semi-log idealization, $e_{cs} = \Gamma - \lambda_e \cdot \ln(p')$; and the a, b, and c coefficients, for a curved CSL represented by a power law function, $e_{cs} = a - b(p'/p_{atm})^c$. The IOD also includes the stress ratio at critical state (M_{tc}), with the subscript "tc" denoting the triaxial compression conditions, estimated as the slope of the line that joins the ultimate points in p' (mean effective stress) versus q (deviatoric stress) plots.

Figure 1a illustrates the particle size distribution (PSD) of the IOD, categorized based on their FC (% passing the #200 sieve) into two groups: those with FC higher ("fine tailings") and lower ("coarse tailings") than 50%. A comparison is drawn with the PSDs of iron ore tailings from the Iron Quadrangle, as compiled by Carneiro et al. (2023). The PSDs of the IOD fall within the "coarse and fine" range (grey area) of the referenced study, with two samples (#4 and #35) falling within the "slimes" range (brown area). Overall, the IOD exhibits a wide range of fine content (FC = 11.8 – 98.7%) and particle diameter (D_{50}= 6.5 – 231.7 μm).

While the majority of IOD samples are typically classified as non-plastic, the iron ore tailings exhibiting plasticity were plotted in the Casagrande plasticity chart (Figure 1b). Samples #33, #34, and #35 demonstrated the highest plasticity, while the remainder exhibited a Plasticity Index (PI) of less than 5%.

Given the distinctive characteristics of iron ore tailings, notably the high G_s values, a dataset comprising the percentage of iron oxide (% hematite) alongside their corresponding G_s values, which ranges from 2.78 to 5.01, was assembled. This data is visualized in Figure 1c, revealing a strong correlation, even when incorporating literature data from Espósito (2000) and Lopes (2000).

The particle shape was assessed using Scanning Electron Microscopy (SEM) images. Most of the IOD tailings exhibit an angular-subangular (A-SA) shape, regardless of the FC. Examples of typical SEM images for different FC are depicted in Figure 1d.

Figure 2a shows the distribution of the CSLs for the IOD plotted over the tailings database by Macedo and Vergaray (2022) (in grey). Overall, the CSLs from the IOD align with those observed in the referenced study. The CSLs cover a broad spectrum in the e versus p' space, the difference in e for a given p' is on the order of 0.40. Half of the CSLs follow a linear relationship (in a semi-log plot). The CSLs from samples #4 and #14 form the upper and lower boundaries for the IOD.

Figure 2b shows a histogram of the M_{tc} values for sands (from Jefferies and Been, 2015), various types of tailings (from Macedo and Vergaray, 2022), and those pertaining to the IOD. The M_{tc} values for mine tailings, including those of the IOD, are generally higher compared to sands. For the IOD, disregarding the lowest value (1.10 from sample #35), this parameter spans from 1.29 to 1.49, with a mean value of 1.37.

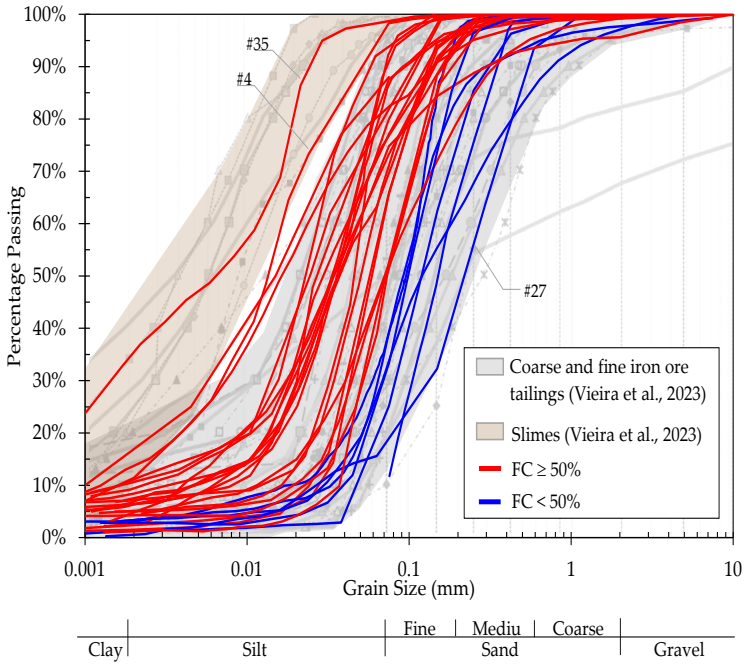

(a) PSD curves of the IOD

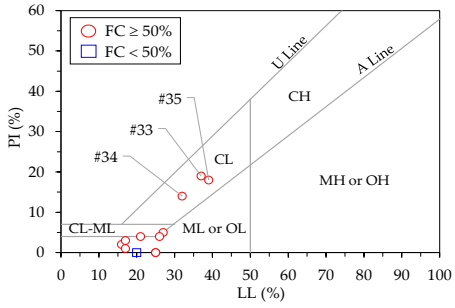

(b) Plasticity of the IOD

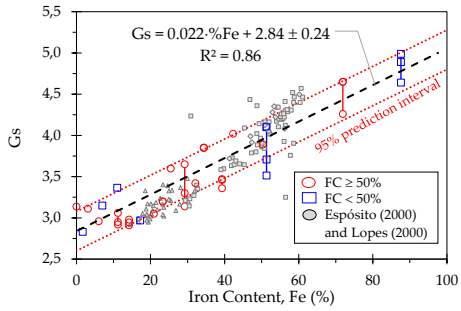

(c) %Fe content

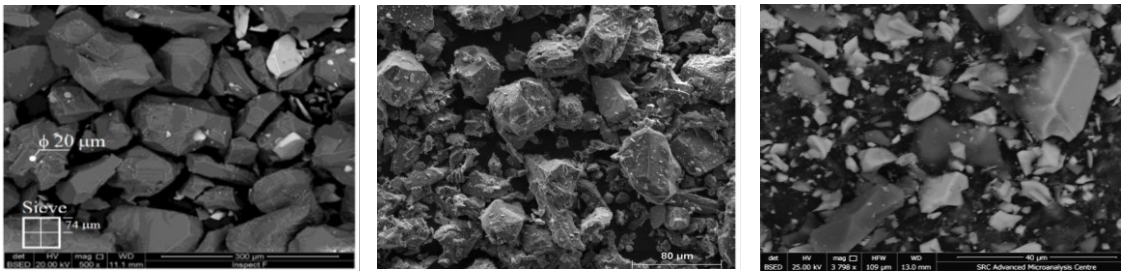

Sample # 16: FC: 33.3% Sample #13: FC: 51.0% Sample #4: FC: 98.3%

(d) SEM images

Figure 1. Index properties of the IOD.

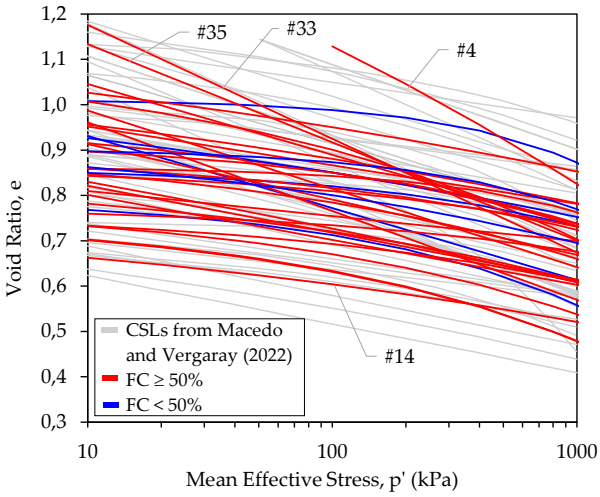

(a) Distribution of the CSLs

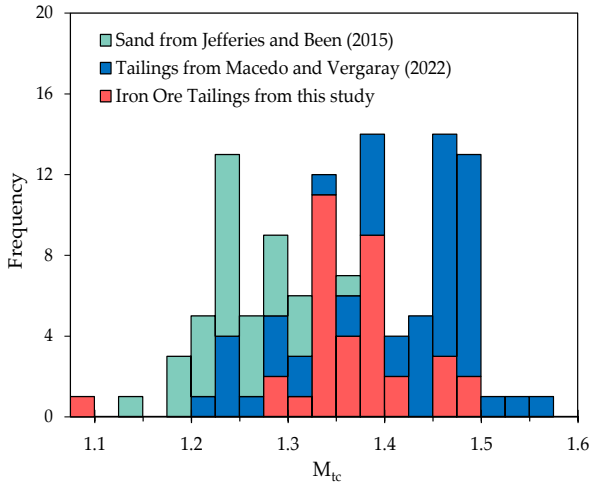

(b) Distribution of the Mtc values

Figure 2. CSL parameters for the IOD

Table 1. Index properties and CSL parameters of the IOD.

ID #	Index properties									Critical state parameters		Source
	D_{50} (µm)	C_u	FC (%)	LL (%)	PI (%)	G_s	Fe (%)	$\boldsymbol{e_{min}}$ | $\boldsymbol{e_{max}}$	Part. Shape	Γ| λ_e or a| b| c	M_{tc}	
1	121	2.9	25.1	-	NP	3.52	51.3	0.99|0.60	A-SA	0.905|0.032|0.63	1.37	This study
2	63	2.5	65.6	-	NP	3.64	NA	0.99|0.54	A-SA	0.870|0.061|0.360	1.35	This study
3	61	2.9	65.9	-	NP	3.70	NA	1.03|0.52	A-SA	0.896|0.080|0.334	1.35	This study
4	14	9.9	98.3	-	NP	3.71	NA	2.32|1.34	A-SA	2.110|0.983|0.117	1.38	This study
5	39	11.6	73.3	16	2	3.42	32.1	1.05|0.38	A-SA	0.759|0.126|0.350	1.37	This study
6	30	25.7	77.1	17	3	3.30	29.2	1.24|0.37	A-SA	0.760|0.129|0.340	1.33	This study
7	25	13.5	74.9	17	1	3.46	39.3	1.32|0.37	A-SA	0.755|0.090|0.355	1.29	This study
8	28	5.0	87.6	-	NP	4.65	71.9	1.30|0.68	A-SA	0.863|0.020|0.700	1.49	This study
9	41	16.7	74.8	-	NP	3.85	34.4	1.23|0.61	A-SA	0.930|0.080|0.380	1.49	This study
10	72	4.9	51.6	20	4	4.38	NA	NA	NA	1.040|0.039	1.38	Robertson et al. (2019)
11	51	4.8	70.8	21	4	3.89	50.3	NA	NA	1.120|0.039	1.38	Robertson et al. (2019)
12	120	6.1	33.7	-	NP	4.89	87.6	NA	A-SA	1.020|0.039	1.38	Robertson et al. (2019)
13	73	4.2	51.0	-	NP	2.95	11.2	1.13|0.48	A-SA	0.865|0.024	1.33	Morgenstern et al. (2016)
14	34	25.4	90.8	-	NP	3.20	23.3	1.18|0.60	NA	0.805|0.201|0.150	1.38	Carneiro (2021)
15	73	5.8	52.2	-	NP	3.05	20.9	1.28|0.51	A-SA	0.770|0.077|0.320	1.40	Oliveira (2022), Wagner et al. (2022), Consoli (2023b), Silva et al. (2024)
16	104	2.7	33.3	-	NP	2.97	17.2	0.99|0.51	A-SA	0.864|0.044|0.480	1.35	
17	96	6.3	39.1	-	NP	2.83	1.7	1.08|0.50	NA	1.000|0.150|0.245	1.30	Consoli (2023a)
18	36	9.6	86.5	-	NP	4.02	42.3	1.09|0.57	NA	0.950|0.150|0.232	1.35	Consoli (2023a)
19	92	3.3	39.1	-	NP	5.01	NA	1.33|0.63	NA	1.012|0.024|0.770	1.35	Cella and Padovani (2021)
20	34	9.2	76.7	-	NP	3.99	NA	1.37|0.71	NA	1.202|0.068	1.33	Cella and Padovani (2021)
21	72	2.5	52.1	-	NP	2.91	14.2	0.85|0.40	A-SA	0.780|0.046|0.355	1.31	Dawson et al. (2019)

ID #	Index properties									Critical state parameters		Source
	D_{50} (μm)	C_u	FC (%)	LL (%)	PI (%)	G_s	Fe (%)	e_{min} | e_{max}	Part. Shape	Γ| λ_e or a| b| c	M_{tc}	
22	46	3.1	79.9	-	NP	3.60	25.4	1.31|0.65	A-SA	1.130|0.230|0.270	1.35	Silva et al. (2022)
23	36	6.2	92.4	-	NP	4.55	NA	NA	NA	1.037|0.037	1.40	Faria et al. (2024)
24	151	3.0	11.8	-	NP	3.15	7.0	NA	NA	1.090|0.069	1.35	Carrizo et al. (2023)
25	23	6.8	93.3	25	NP	3.11	3.1	1.21|0.69	A-SA	1.157|0.085	1.40	Li and Coop (2019)
26	38	8.7	67.6	25	NP	3.14	0.0	1.10|0.59	A-SA	0.912|0.128|0.296	1.36	Li and Coop (2019)
27	232	10.4	17.9	20	NP	3.37	11.0	1.09|0.49	A-SA	0.799|0.087|0.445	1.41	Li and Coop (2019)
28	15	23.5	88.0	-	NP	2.78	NA	NA	NA	0.864|0.144|0.243	1.46	Reid et. al. (2018)
29	16	18.9	82.3	-	NP	2.96	6.0	NA	A-SA	1.539|0.813|0.059	1.39	Reid and Fanni (2020)
30	NA	NA	NA	27	5	2.99	NA	NA	NA	0.900|0.043	1.47	Smith et al. (2019)
31	NA	NA	NA	26	4	3.23	NA	NA	NA	1.035|0.053	1.33	Smith et al. (2019)
32	NA	NA	NA	-	NP	2.96	NA	NA	NA	0.925|0.045	1.42	Smith et al. (2019)
33	NA	NA	NA	37	19	3.75	NA	NA	NA	1.427|0.109	1.47	Smith et al. (2019)
34	NA	NA	NA	32	14	3.46	NA	NA	NA	1.160|0.075	1.33	Smith et al. (2019)
35	7	33.4	98.7	39	18	3.71	NA	NA	NA	1.350|0.094	1.10	Mmbando et al. (2023)

Notes:
1) NA: data not available, NP: Non-plastic, FC: Fines content, C_u: Coefficient of uniformity, D_{50}: Mean particle size, LL: Liquid limit, PI: Plasticity index, Fe: Iron oxide content, e_{min}, e_{max}: minimum and maximum void ratio, A: Angular, SA: Subangular, M_{tc}: Stress ratio at critical state
2) Tailings 10 to 13 represent results from the Fundão and Brumadinho tailings failures.
3) Tailings 14 to 17 are results from filtered tailings samples.
4) $a, b,$ and c parameters are reported in cases where CSL fits a curve, while Γ and λ_e are reported for the conventional linear approach.
5) Tailings 35 exhibited two CSL values depending on the sample preparation method (slurry deposition and moist tamping). The results obtained through moist tamping were selected for inclusion in the database.

3 EVALUATION OF TRENDS AND CORRELATIONS

A review of trends and correlations between CS parameters (Γ, λ_e and M_{tc}) and index properties was conducted. To investigate the influence of the PSD, three key material characteristics (D_{50}, FC and C_u) were evaluated. Plasticity was assessed via Atterberg limits (PI and LL), material state through void ratio (e_{min} and e_{max}) and mineralogy by considering the iron oxide (%Fe) content.

For the 'curved' CSLs with minimal curvature, a void ratio deviation of less than 0.02 over the stress range of p' = 30 – 900kPa, which typically encompasses the range of interest for most geotechnical TSF projects, a common semi-logarithmic representation was adopted for comparison purposes.

Figure 3 displays a series of charts illustrating acceptable trends observed in the comparison between CSL and soil index parameters. When available, data from the 'literature' on other tailings and/or natural soils have also been incorporated into these figures for comparison. Of note, λ_e and λ_{10} will be used interchangeably, depending on the availability of the literature data used for comparisons.

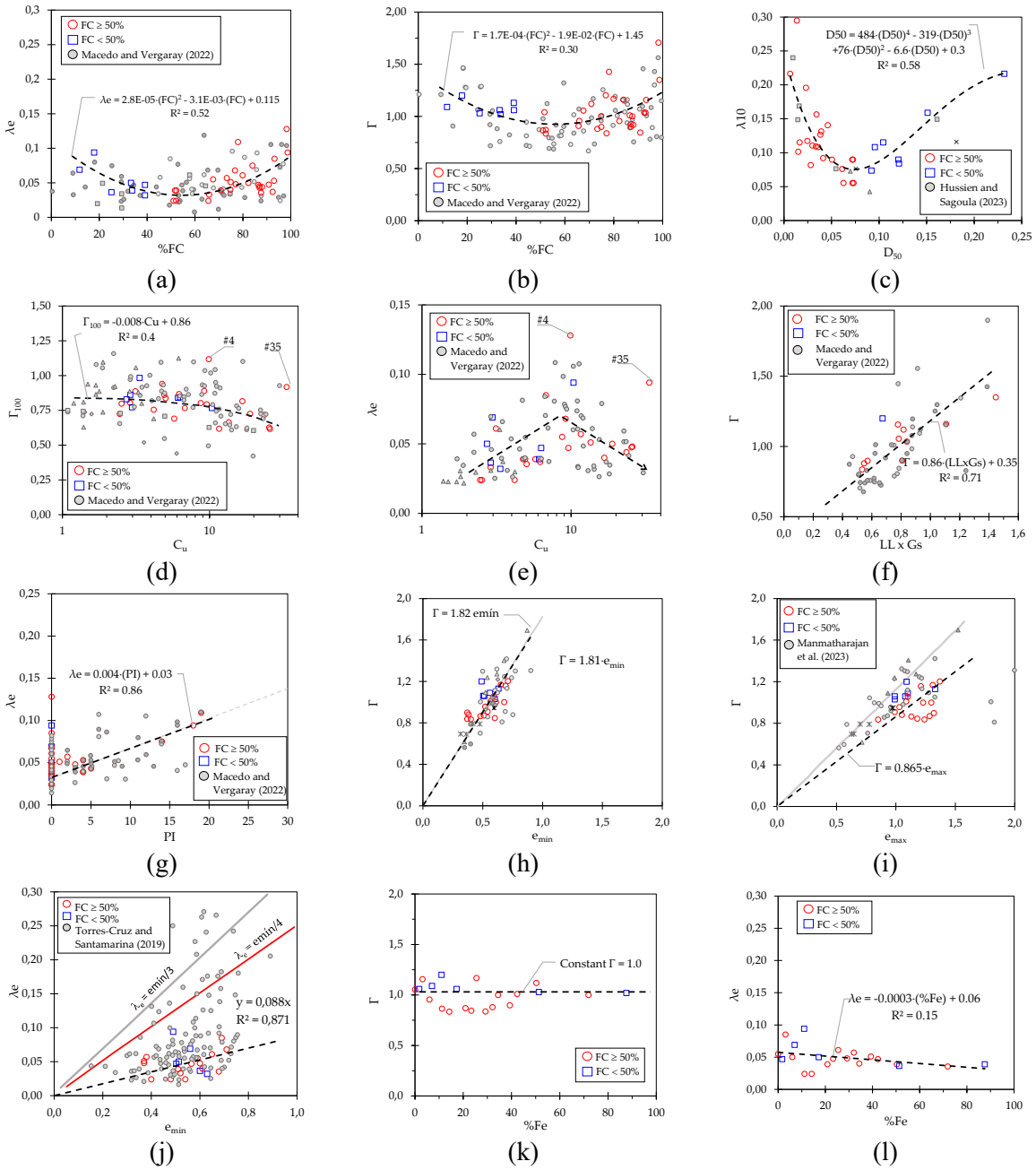

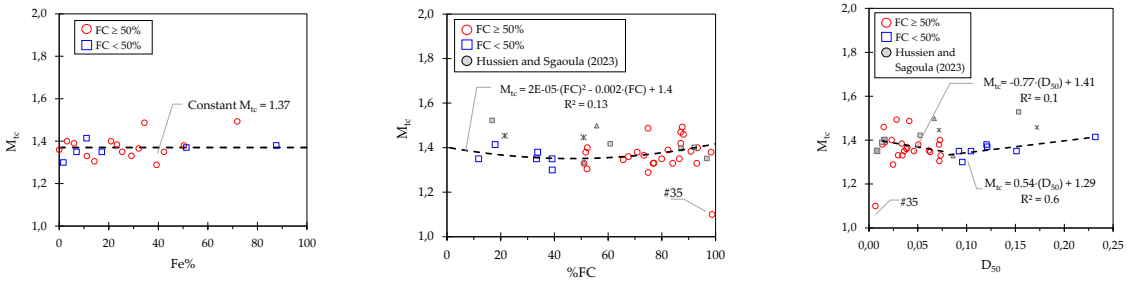

(m) (n) (o)

Figure 3. Evaluation of trends and correlations for the IOD.

Based on the figures, the following can be highlighted:

- Both Γ and λ_e exhibit a low to moderate correlation with FC (Figures 3a, 3b), with Γ decreasing as FC increases until it reaches approximately 50% of FC (or in other terms, when D_{50} is ~0.075mm), after which this trend reverses. This pattern is consistent with findings from published studies, such as Smith et al. (2019), Macedo and Vergaray (2022), and Manmatharajan et al. (2023). The U-shaped trend can be attributed to the behavior of finer particles filling the voids: below 50% FC, the tailings are dominated by a sand skeleton, while above 50%, contacts are primarily influenced by silt and clay-sized particles. At around 50% FC, the finer fraction filling the voids contributes to the load-carrying skeleton, resulting in a less compressible material (i.e., lower λ_e).
- D_{50} exhibits a moderate relationship with λ_{10} (Figure 3c) and Γ (not depicted here). The trend follows a V-shaped curvature, with λ_{10} sharply decreasing as D_{50} increases until reaching approximately 0.075 mm, consistent with the observations in Figures 3a, 3b. Beyond this point, the trend reverses, showing a smooth positive linear relationship.
- Figure 3d depicts the impact of material grading (using C_u as a proxy) on Γ, presented in an alternative form as Γ_{100} (i.e., the altitude of the CSL at 100kPa) as proposed by Torrez-Cruz and Santamarina (2019). The observed linear trend suggests a decrease in Γ as C_u increases. The IOD values fall within the range of results from other tests on different types of tailings and sands with lower roundness (as compiled by Macedo and Vergaray, 2022) (plotted in grey), typically characterizing the tailings of the IOD (see Figure 1d).
- Figure 3e shows λ_e in terms of C_u. It is noted that λ_e tends to increase with C_u up to values on the order of 6-8 and then decreases as C_u keeps increasing following a similar trend as showed in Macedo and Vergaray (2022). This observation suggests an enhanced particle packing with high C_u, consistent with classical criteria for classification of 'well-graded' sand by the Unified Soil Classification System (USCS), which states that a more densely packed arrangement of particles can be achieved when C_u is greater than 6 and C_c (coefficient of curvature) is between 1 and 3.
- While the available data on iron ore tailings with Atterberg limits are limited, the available results suggest a strong linear correlation between Γ and LL when normalized by specific gravity $LLxGs$ (see Figure 3f), a trend also observed by Macedo and Vergaray (2022) and Smith et al. (2019). This correlation aligns with concepts from the CSSM framework, as outlined by Schofield and Wroth (1968). Similarly, a linear correlation was observed between PI and λ_e (see Figure 3g). This outcome is expected, given that both parameters serve as proxies for compressibility, in line with CSSM-based concepts.
- The spatial variability of e_{min} within a tailings deposit anticipates spatial variability of Γ, given the good correlation between these parameters (see Figure 3h). This correlation extends to other datasets of natural soils and various types of tailings (from Manmatharajan et al., 2023), as depicted in grey in Figure 3h. Similarly, a good linear trend was observed between e_{max} and Γ (see Figure 3i). However, the slope of the linear regression for iron ore tailings is lower compared to tailings from other commodities or natural soil. It appears that iron ore tailings tend to exhibit lower Γ values than other materials for a given e_{max}.

- The range of possible λ_e values increase with e_{min} (see Figure 3j). Overall, the expected λ_e values are lower than $e_{min}/4$. The data from IOD falls within the range of most of other quartz-rich tailings (plotted in grey) based on the Torrez-Cruz and Santamarina (2020) database.
- Figures 3k, 3l and 3m, suggest that the iron oxide content (% hematite) does not exert a significant influence on λ_e, Γ or M_{tc}, with only a weak linear trend observed for λ_e.
- Broader investigations by Torres-Cruz and Santamarina (2020), encompassing soils beyond tailings, suggest that the primary factor influencing M_{tc} is neither mineralogy nor particle size, but particle shape. While this study finds no significant variation in particle shape among the examined tailings, a wide range of M_{tc} values was observed within the IOD. Upon examining M_{tc} values alongside index properties, it was observed that, despite weak to moderate correlations, there may be a potential influence of FC (Figure 3n) and D_{50} (Figure 3o). These trends exhibit similar U-shaped patterns as seen in Figures 3a to 3c.
- Caution is advised when analyzing very fine iron ore tailings (slimes) (refer to Figure 1a). In certain instances, such as with samples #4 and #35 in Figures 3d, 3e, the results for these samples are outliers when compared to other 'Fine and Coarse' iron ore tailings.

4 CONCLUSIONS

In this article, we compared CSL parameters (Γ, λ_e and M_{tc}) inferred from laboratory testing of iron ore mine tailings gathered from mine sites in Brazil and globally with their laboratory index properties (G_s, FC, D_{50}, C_u, PI, LL, e_{min}, e_{max} and iron oxide content). We considered an equivalent 'linear' function using a semi-log idealization for 'curved' CSLs within the stress range of p' = 30 – 900kPa. Our aim was to establish correlations between basic tailings data and CS parameters.

Upon analyzing the results, two primary conclusions emerged. Firstly, the observed trends using 35 CSLs did not exhibit significant different behavior than other types of tailings. This is evident when examining correlations with index properties such as FC, D_{50}, C_u, plasticity, and void ratio, which displayed a greater potential to influence CSL parameters compared to correlations with iron oxide content. This suggests that inferences about tailings behavior made from other types of tailings can be reasonably adopted.

The second finding is that, when particle shape remains consistent, as observed in this study for the IOD, certain index parameters such as FC and D_{50} may exert a slight influence on M_{tc} values.

ACKNOWLEDGEMENTS

The authors would like to acknowledge Daniel Klassen from KCB Canada, for his assistance in reviewing this paper.

REFERENCES

Carneiro, J. J. V. (2021) *Characterization and Behaviour of Iron Ore Tailings: The Effect of Compaction And Stresses*, Dissertation (Master's Degree in Civil Engineering) - Federal University of Viçosa - UFV, Viçosa.

Carneiro, J. J. V.; Marques, E. A. G.; Fonseca, A. J. P. V.; Oliveira, A. H. C. (2023) *Characterization of an Iron Ore Tailing Sample and the Evaluation of Its Representativeness*. Geotechnical and Geological Engineering, Springer, p. 2833 – 2852.

Carrizo, L.; Tasso, N.; Sottile, M. (2023*) Caracterización geotécnica de un relave minero susceptible a licuar: Geotechnical characterization of a mine tailings susceptible to liquefaction*, XXVI Congreso Argentino de Mecánica de Suelos e Ingeniería Geotécnica, Comodoro: Rivadavia, 6p.

Cella, P. R. C.; Padovani, F. A. (2021) *Five Brazilian Tailings – from laboratory and field data towards safer design criteria*, 7th Internacional Conference Tailings Management, virtual event, 29p.

Consoli, N. C. (2023) (a) *Critical State Analysis of Two Compacted Filtered Iron Ore Tailings with Different Granding and Mineralogy at Different Stages of Treatment*. Acta Geotechnica, Springer, p. 881-898, DOI: 10.1007/s11440-023-01963-9.

Consoli, N. C. (2023) (b) *Determination of critical state line (CSL) for silty-sandy iron ore tailings subjected to low-high confining pressures*, Journal of Rock Mechanics and Geotechnical Engineering, 18p, DOI: 10.1016/j.jrmge.2023.06.014.

Dawson, R.; Burgin, A.; Macowich, M.; Bernardo, J.; Vasconcelos, A. (2019). *Laboratory and CPTu Characterization of Samarco Sand Tailings*, Tailings and Mine Waste. Vancouver, Canada.13p.

Espósito, T. J (2000). *Metodologia Probabilística e Observacional Aplicada a Barragens de Rejeito Construídas por Aterro Hidráulico*. Universidade de Brasília. Brasília, BR.

Faria, A. O.; Delgado, B. G.; Ferreira, L. D.; Junior, M. P. S. (2024) *Comparative evaluation of constitutive models for stress-strain analysis of an iron ore tailings from the Quadrilátero Ferrífero, Minas Gerais, Brazil*. Soils and Rocks: An International Journal of Geotechnical and Geoenvironmental Engineering, 12p, DOI: 10.28927/SR.2024.011022.

Hussien, M. N And Sgaoula, J. (2023) *Tailings State from Basic Laboratory Tests and CPT Data,* Proceedings of Tailings and Mine Waste. Vancouver, Canada, 14p.

Jefferies, M. And Been, K. (2015) *Soil Liquefaction: A Critical State Approach*. 2. ed. Taylor & Francis Group. London, UK.

Lade, P.V. And Yamamuro, J.A. (1997) *Effects of Non-Plastic Fines on Static Liquefaction of Sands*. Canadian Geotechnical Journal, p. 918 – 928, DOI: 10.1139/cgj-34-6-918.

Li, W.; Coop, M. R. (2019) *Mechanical behaviour of Panzhihua iron tailings*. Canadian Geotechnical Journal, 16p, DOI: 10.1139/cgj-2018-0032.

Lopes, M. C. O. (2000). *Disposição hidráulica de rejeitos arenosos e influência nos parâmetros de resistência*. University of Brasília. Brasília, BR, 157p.

Macedo, J. And Vergaray, L. (2022) *Properties of mine tailings for static liquefaction assessment.* Canadian Geotechnical Journal, Canada, 21p.

Manmatharajan, M. V.; Gill, S.; Liu, W.; Ingabire, E. P.; Sy, A.; Ghafghazi, M. (2023) *Effect of particle size and particle size distribution on critical state loci of granular soils*. Canadian Geotechnical Journal, DOI: 10.1139/cgj-2021-0643.

Mmbando, E.; Fourie, A.; Reid, D. (2023) *Mechanics of an Iron Ore Tailings Exhibiting Transitional Behaviour*. Geotechnical and Geological Engineering, Springer, 10 p, DOI: 10.1007/s10706-023-02379-8.

Morgenstern, N. R.; Vick, S. G.; Viotti, C. B.; Watts, B. D. (2016). *Report on the Immediate Causes of the Failure of the Fundão Dam.* Fundão Tailings Dam Review Panel.

Oliveira, S. C. (2022). *Influência do Estado de Tensão na Obtenção dos Parâmetros de Estado Crítico de Rejeitos Filtrados de Minério de Ferro*. Universidade Federal de Ouro Preto. Ouro Preto, BR.

Reid, D.; Fanni, R.; Koh, K.; Orea, I. (2018). *Characterisation of a subaqueously deposited silt iron ore tailings*. Geotechnique Letters 8, 278-283. DOI: 10.1680.

Reid, D.; Fanni, R. (2020) *A comparison of intact and reconstituted samples of a silt tailings*. Geotechnique, 45p, DOI: 10.1680/jgeot.20.P.020.

Robertson, P. K.; Melo, L.; Williams, D. J.; Wilson, G. W. (2019) *Report of the Expert Panel on the Technical Causes of the Failure of Feijão Dam I*. Expert Panel.

Schofield, A., And Wroth, P. (1968) *Critical State Soil Mechanics*, 1 Ed., McGraw-Hill

Silva, J. P. S.; Cacciari, P. P.; Torres, V. F. N.; Ribeiro, L. F. M.; Assis, A. P. (2022) *Behavioural analysis of iron ore tailings through critical state soil mechanics*. Soils and Rocks, 13p, DOI: 10.28927/SR.2022.071921.

Silva, J. P. S., Rissoli, A. L. C., Cacciari, P. P., Fonseca, A. J. P. V., Scheuermann, H. C., Wagner, A. C., Carvalho, J. V. A., Festugato, L., Consoli, N. C. (2024) *Triaxial testing response of compacted iron ore tailings considering a broad spectrum of confining pressures*. Soils and Foundations, Volume 64, Issue 2.

Smith, K.; Fanni, R.; Reid, D. (2019) *Critical State Testing of Tailings - Comparison between Various Tailings and Implications for Design*. In: Proceedings of Tailings and Mine Waste. Vancouver, Canada, 14p.

Torrez-Cruz, L. A.; Santamarina J. C. (2020). *The critical state line of nonplastic tailings*. Canadian Geotechnical Journal. Vancouver, Canada, p. 1508-1517. DOI: 10.1139/cgj-2019-0019.

Wagner, A. C.; Silva, J. P. S.; Carvalho, J. V. A.; Rissoli, A. L. C.; Cacciari, P. P.; Chaves, H. M., Scheuermann, H. C.; Consoli, N. C. (2022) *Mechanical behavior of iron ore tailings under standard compression and extension triaxial stress paths*. Journal of Rock Mechanics and Geotechnical Engineering, p. 1883-1894, DOI: 10.1016/j.jrmge.2022.11.013.